Shock-wave-based density down ramp for electron injection

Chunmei Wang,[1,*] Ji Li,[2] Jun Sun,[1] and Xisheng Luo[2]

[1]*School of Mechanical and Automotive Engineering, Hefei University of Technology, Postcode 230009, Hefei, China*
[2]*Department of Modern Mechanics, University of Science and Technology of China, Hefei, China*

(Received 30 August 2011; published 2 February 2012)

We demonstrate a sharp density transition for electron injection in laser wakefield acceleration through numerical study. This density transition is generated by a detached shock wave induced by a cylinder inserted into a supersonic helium gas flow. In a Mach 1.5 flow, the scale length of the density transition L_{grad} can approximately equal to plasma wavelength λ_p at the shock front, and can be further reduced with an increase of the flow Mach number. A density down ramp with $L_{\mathrm{grad}} \geq \lambda_p$ can reduce the phase velocity of the wakefield and lower the energy threshold for the electrons to be trapped. Moreover, the quality of the accelerated beam may be greatly improved by precisely controlling of L_{grad} to be one λ_p. For an even sharper density down ramp with $L_{\mathrm{grad}} \ll \lambda_p$, the oscillating electrons in the plasma wave will up shift their phase when crossing the ramp, therefore a fraction of the electrons are injected into the accelerating field. For this injection mechanism, there is no threshold requirement for the pump laser intensity to reach wave breaking, which is a big advantage as compared with other injection mechanisms.

DOI: 10.1103/PhysRevSTAB.15.020401 PACS numbers: 52.38.Kd, 42.65.Jx, 41.75.Jv

I. INTRODUCTION

In laser wakefield accelerators (LWFA), a wakefield driven by a high intensity laser can sustain an extremely high electric field up to 100 GV/m, 3 orders of magnitude larger than those obtained in conventional radio-frequency linear accelerators [1]. LWFA typically have a density of 10^{18}–10^{19} cm^{-3}, and a plasma wavelength λ_p of 30–10 μm. If an electron bunch is injected into a wakefield such that it is accelerated while maintaining a small energy spread, then it is necessary for the bunch to be a fraction of λ_p and located at the appropriate phase of the wakefield with sufficient initial energy. This requires the femtosecond electron bunch to be injected with femtosecond timing accuracy.

Several ways can fulfill these requirements and realize the injection of electrons: (1) self-injection in the so-called bubble region; (2) optical injection by colliding laser beams; (3) injection in a density down ramp.

The most basic and simplest method of injection is the self-trapping in the so-called bubble region [2,3]. When a laser pulse has a duration $\tau \geq \lambda_p/c$, it will undergo self-focusing and compression until the resonant condition is met, resulting in a large amplitude nonlinear plasma wave. The pulse can evolve into a state where its ponderomotive force causes electron cavitation. As the radially expelled electrons flow along the cavity boundary and collide at the bubble base, transverse breaking occurs and a bunch of electrons are injected into the plasma wave. These electrons produce a field that terminates further injection of electrons and damps the plasma wave, resulting in very localized injection and thus formation of a monoenergetic electron beam. This phenomenon was observed and monoenergetic beams were reported for the first time in 2004 [4–6]. However, in the self-injection experiment, injection and acceleration are interdependent, which limits tunability and control of the bunch quality. The monoenergetic electron bunch was only observed in a narrow parameter window.

Optical injection by colliding counterpropagating laser pulses has been demonstrated experimentally [7,8], resulting in stable, high quality, and tunable electron beams [9]. This approach works well but is not easy to implement experimentally. The multiple laser beams are required to be synchronized at femtosecond level and overlapped at micrometer level.

Injection in a downward density ramp could be a promising way as it does not involve temporal and spatial restriction on the laser beams; it is easier to implement experimentally. Injection by phase upshift of the background electrons in a very sharp density down ramp ($L_{\mathrm{grad}} \ll \lambda_p$) has been proposed by Suk *et al.* [10]. This injection process can be described in a simple picture. Electrons in the low density region have a long oscillation period; when these electrons pass the boundary into the high density region where electrons experience short oscillation period, the intruders are forced to oscillate faster. When they return to the low density region, their wave phase is ahead of the electrons remaining in this region and thus become trapped. For significant injection to occur, the plasma must have a sudden density transition with $L_{\mathrm{grad}} \ll \lambda_p$. Theoretically, this is a very effective way for control

*chunmei.wang@hotmail.com

injection since it is not necessary for the pump laser intensity to reach wave breaking. However, a sharp density transition is not the easiest to implement experimentally. The commonly used laser heating method shows their weakness in realizing a very sharp density transition [11,12], and a density down ramp with $L_{\mathrm{grad}} < \lambda_p$ is not yet demonstrated experimentally.

Bulanov [13] proposed an injection method by lowering the threshold for trapping the plasma background electrons in a density down ramp with $L_{\mathrm{grad}} > \lambda_p$. The phase velocity of the plasma wave is slowing down at the density ramp and can be expressed as [14]

$$\frac{v_p}{c} = \left(1 + \frac{\zeta}{k_p}\frac{dk_p}{dz}\right)^{-1}, \tag{1}$$

where $\zeta = z - ct$ and $k_p(z)$ depends on z through the plasma electron density $n_e(z)$ and $dk_p/dz = (k_p/2n_e) \times (dn_e/dz)$. From the above equation, one can see that, for a down ramp density $dn_e/dz < 0$ behind the pulse, $\zeta < 0$, the phase velocity v_p slows down. The minimum energy an electron needs to be trapped in a wakefield of amplitude $\Delta\varphi$ is given by

$$\gamma_{\min} = \gamma_p(1 + \gamma_p\Delta\phi) - \sqrt{\gamma_p^2(1 + \gamma_p\Delta\phi)^2 - (\gamma_p^2 + \gamma_p^2\Delta\phi^2 + 2\gamma_p\Delta\phi)}, \tag{2}$$

where $\gamma_p = (1 - v_p^2/c^2)^{-1/2}$ is the Lorentz factor associated to the phase velocity of the plasma wave, $\Delta\varphi = \varphi_{\max} - \varphi_{\min}$ is the wakefield amplitude in focusing and accelerating phases. For a given $\Delta\varphi$, the threshold for trapping decreases as γ_p decreases. A decreasing plasma density slows down the phase velocity of the plasma wave, which reduces the threshold for trapping by reducing the velocity that the electrons must achieve to be trapped. For the injection to occur, it was shown that the density transition could have a scale length $L_{\mathrm{grad}} \geq \lambda_p$ [13].

Making use of a Gaussian density distribution of a gas jet, Geddes [15] achieved a density ramp by focusing a laser pulse at the downstream of the gas jet transverse to the pump pulse. The scale length of the density down ramp, depending on the initial density profile of the gas jet, is almost unchangeable unless one can change the jet profile. The L_{grad} obtained by Geddes is about 100 μm, 10 times longer than $\lambda_p(\approx 10\ \mu\mathrm{m})$. By using this density ramp, a rather stable injection performance was demonstrated. Recently, the gas jet implemented via a laser machined nozzle and a capillary separated trapping and acceleration, and gave excellent charge and energy stability [16]. Faure *et al.* [17] shorten L_{grad} to 30 μm by using an intense laser ($I = 1.5 \times 10^{17}$ W/cm^2) to heat a helium gas jet ($n_e = 10^{19}$ cm^{-3}) transversely. A density ramp was formed during the plasma expansion process. This 30 μm scale length can give simultaneously low energy spread, good emittance, and stable performance.

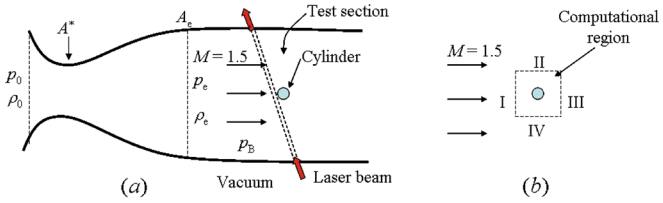

FIG. 1. (a) Schematic diagram of a supersonic nozzle and a cylinder inserted laterally into the supersonic flow to generate a detached shock. (b) Computational region of the gas flow.

Different from the laser heating method, here we propose a shock wave scheme to achieve a sharp density ramp required by the injection methods of Suk [10] and Bulanov [13]. Suggested by Schmid's work [18], a detached shock is generated by introducing a cylinder into a supersonic helium gas flow. The flow variables including the density have a big jump at the shock front. This jump happens within a distance roughly 1 order of magnitude larger than the molecular mean-free path, which means that we can have a density ramp within a few micrometers (for helium gas with density of 10^{19} cm^{-3}).

II. METHOD FOR THE GENERATION OF A SHARP DENSITY RAMP

To generate a shock wave, the gas flow must be supersonic. Figure 1(a) shows schematically the setup for the generation of a uniform supersonic flow [19]. We first study a modest supersonic flow with a Mach number $M = 1.5$. A convergent-divergent nozzle with an area ratio of the exit to a throat $A_e/A^* = 1.176$ is used. Moreover, we need to establish a pressure ratio of the nozzle inlet to the exit, $p_0/p_e = 3.671$, a temperature ratio, $T_0/T_e = 1.45$, across the nozzle to obtain a free jet to $M = 1.5$ at the exit. In order to achieve a 1.735×10^4 Pa and 250 K supersonic flow at the nozzle exit (the corresponding helium number density $n_{\mathrm{He}} = 5 \times 10^{18}$ cm^{-3}), we need a reservoir with a pressure $p_0 = 6.47 \times 10^4$ Pa and a temperature $T_0 = 362.5$ K at the inlet to the nozzle. The nozzle is smoothly connected to a tunnel. The back pressure p_B at the nozzle exit must be kept at 1.735×10^4 Pa which is essential in achieving a uniform supersonic flow. Directly exposing the nozzle to a vacuum will result in jet expansion. Once formed, the uniform supersonic gas flows in the tunnel where a cylinder is inserted laterally to block the flow and induce a detached shock wave. The pump laser beam is sent from the vacuum into the test section through side windows of the tunnel (see Fig. 1).

III. SIMULATION RESULTS

The computational domain used for modeling a uniform supersonic helium gas passing a cylinder is shown in

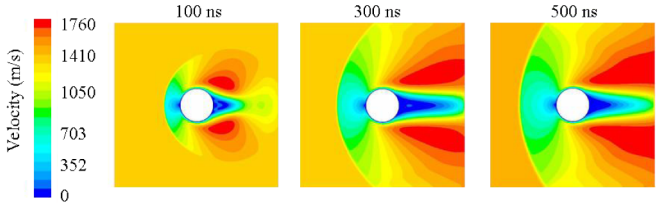

FIG. 2. The evolution of the velocity 100, 300, and 500 ns after inserting a cylinder into a Mach 1.5 free stream.

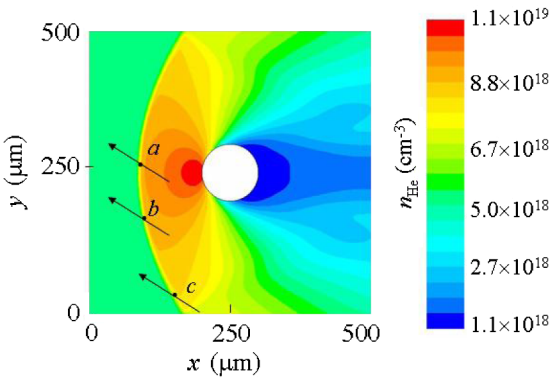

FIG. 3. The density contour 500 ns after inserting the cylinder into the supersonic helium gas flow, corresponding to the last snapshot of velocity shown in Fig. 2. Arrows indicate laser propagation direction.

Fig. 1(b), which is a 500×500 μm dashed box. The 2D box is separated into 49 000 cells. The radius R of the cylinder is 50 μm. Boundaries I, II, III, and IV are defined as pressure far-field boundaries, and the cylinder surface is defined as a solid wall. The pressure far-field condition is a characteristic boundary condition; it uses characteristic information (Riemann invariants) to determine the flow variables at the boundary. Two-dimensional Navier-Stokes equations are employed in our simulation. The governing equations are numerically solved by the finite volume method; a 2nd order upwind scheme is used for spatial discretization of the flow. Temporal integration is performed using an implicit method. For the residual monitors, the convergence criterion is set to be 10^{-4}; only when the errors is reduced to 10^{-4} can the simulation go to the next time step. For this physical problem, my co-authors from the shock wave group at USTC and I studied independently with two computational fluid dynamics codes, and we arrive at the same results.

Figure 2 shows the calculated velocity contours 100, 300, and 500 ns after inserting the cylinder into the flow. A curved bow shock stands a distance in front of the cylinder, and moves away from the solid cylinder with time. The three snapshots show a similar feature: in front of the cylinder nose, the velocity drops dramatically to subsonic flow (the initial local sound speed is 925.6 m/s), away from the nose region, the shock wave gradually becomes curved and weaker, eventually evolving into supersonic flow at large distances from the cylinder.

Figure 3 shows the density contour 500 ns after inserting the cylinder into the supersonic flow. In front of the shock, the flow has a uniform density $n_{\mathrm{He}} = 5 \times 10^{18}$ cm^{-3}. Point a corresponds to a normal shock wave, the density jump is strong there. The shock at point c becomes relatively weak. The arrows in Fig. 3 indicate the pump laser propagation direction. Supposing that the laser propagates at 40° to the horizontal through points a, b, and c (see Fig. 3), the laser pulse will experience different density ramps which are shown in Figs. 4(a)–4(c), respectively. In Fig. 4(a), the density decreases slowly from 1.1×10^{19} to 9×10^{18} cm^{-3}, and then suddenly drops to 5×10^{18} cm^{-3} within 10 μm in the $-x$ direction, so that the laser experiences a sharp density down ramp within 13 μm. In Fig. 4(b), the density experiences a density plateau, and then drops from 9×10^{18} to 5×10^{18} cm^{-3} within 10 μm in the $-x$ direction, this plateau has a width of around 100 μm [Fig. 4(b) only shows part of the plateau]. The scale lengths L_{grad} along arrows a and b are in between a double ionized ($n_e = 1.0 \times 10^{19}$ cm^{-3}) plasma wave length (~ 10 μm), and are slightly shorter than a single ionized ($n_e = 5 \times 10^{18}$ cm^{-3}) plasma wave length (~ 15 μm). In Fig. 4(c), the density drops from 7.8×10^{18} to 5×10^{18} cm^{-3} within 15 μm, so the L_{grad} along arrow c is 20 μm, slightly longer than a single ionized plasma wave. The scale lengths of the density ramp in Figs. 4(a)–4(c) are all on the same order of the plasma wave length, $L_{\mathrm{grad}} \sim \lambda_p$. Such density down ramps can reduce the phase velocity of the wakefield and lower the energy threshold for the electrons self-injection. More importantly, the beam quality might be greatly improved in a density down ramp with $L_{\mathrm{grad}} \approx \lambda_p$.

We now increase the flow Mach number to 3. The pressure ratio and the temperature ratio of the nozzle in Fig. 1 have to be changed accordingly. An area ratio $A_e/A^* = 4.235$, a pressure ratio, $p_0/p_e = 36.73$, and a temperature ratio $T_0/T_e = 2.8$ across the nozzle are needed to obtain a Mach 3 flow at the exit. The pressure and the temperature at nozzle outlet are still fixed at 1.735×10^4 Pa and 250 K ($n_{\mathrm{He}} = 5 \times 10^{18}$ cm^{-3}), the same as in the Mach 1.5 case. So the reservoir at the nozzle inlet should have a pressure $p_0 = 6.37 \times 10^5$ Pa and a temperature $T_0 = 700$ K.

The Mach 3 flow reaches steady state much faster than the Mach 1.5 flow. A steady flow is fully developed 200 ns after inserting the cylinder into the helium gas. Thereafter, the shape and location of the shock wave does not change with time. The velocity and density of the steady flow are shown in Fig. 5. The velocity drops dramatically from supersonic to subsonic flow in front of the cylinder nose. Away from the nose region, the shock wave becomes curved and weaker. With the increase of the Mach number, the shock front moves closer to the tip of the cylinder. The

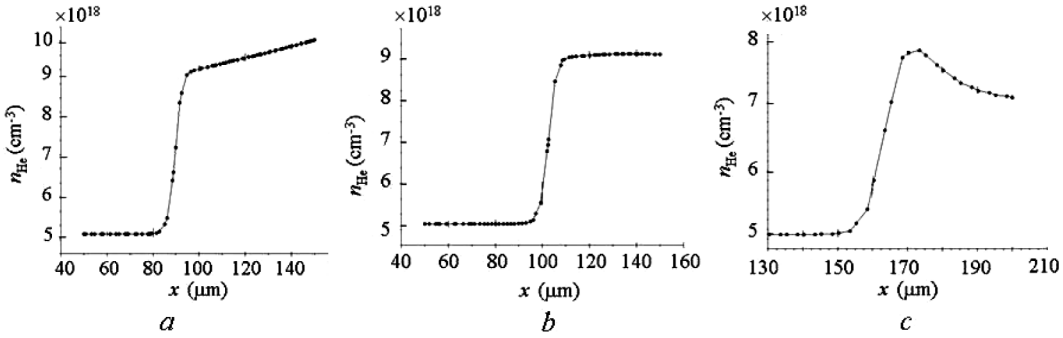

FIG. 4. The density distribution along the x direction through points a (x, $y = 250$), b (x, $y = 150$), and c (x, $y = 50$) of Fig. 3, respectively.

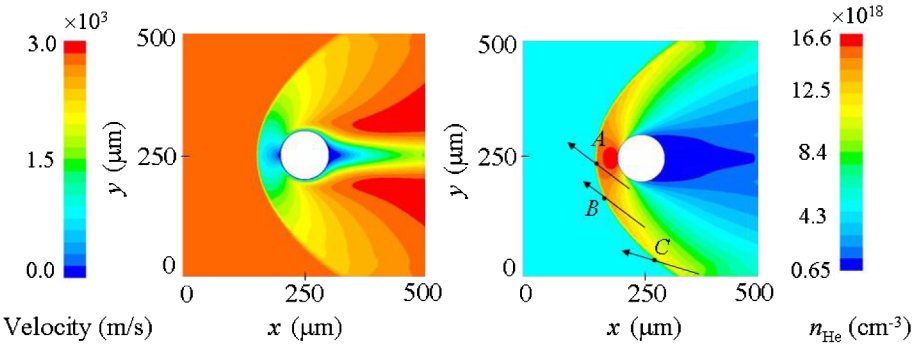

FIG. 5. The contours of the velocity (left frame) and the density (right frame) 200 ns after inserting the cylinders into the Mach 3 flow. Arrows indicate laser propagation direction.

distance δ in between the shock front and the cylinder nose reduced from $2.5R$ in Mach 1.5 case to around $0.8R$ in the Mach 3 case (see Figs. 3 and 5).

Supposing that the laser propagates at 40° to the horizontal through points A and B at 30° to the horizontal through point C (see Fig. 5), the laser pulse will experience different density ramps which are shown in Figs. 6(a)–6(c), respectively. In the frame A, the density drops from 1.5×10^{19} to 5×10^{18} cm^{-3} within 6 μm in the $-x$ direction. So that along the arrow A, L_{grad} is 7.8 μm, $1/2$ of the single ionized plasma wavelength. The density contrast increase from 2 in the Mach 1.5 case to 3 in the Mach 3 case. In the frame B, the density drops from 1.4×10^{19} to 5×10^{18} cm^{-3} within 8 μm in the $-x$ direction, so that L_{grad} along arrow B is 10 μm, and the shock is still very strong. In the frame C, the density drops from 1.2×10^{19} to 5×10^{18} cm^{-3} within 20 μm in the $-x$ direction. Comparing Fig. 4 with Fig. 6, one can see that the Mach 3 flow has greater density contrast and steeper gradient than the Mach 1.5 flow. The shock has a symmetric structure, and away from the cylinder nose, it becomes curved and weaker. If we send a laser at 40° to the horizontal, L_{grad} is shorter than the plasma wavelength in the interval $y = [150\ \mu\text{m}, 350\ \mu\text{m}]$.

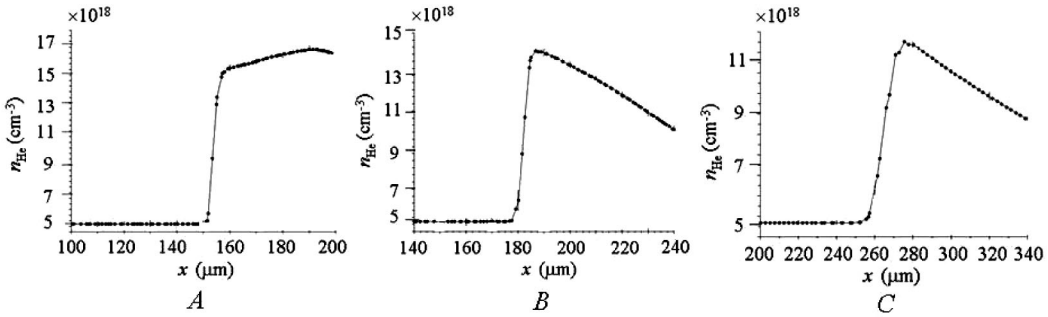

FIG. 6. The density transitions along the x direction through points $A(x, y = 250)$, $B(x, y = 150)$, and $C(x, y = 50)$ of Fig. 5, respectively.

IV. CONCLUSION

The shock structures for Mach 1.5 and Mach 3 flows are studied numerically. A sharp density down ramp is generated in a detached shock wave. Depending on the Mach number and the location in the shock wave, the density gradients with $L_{\mathrm{grad}} \approx \lambda_p$ and $L_{\mathrm{grad}} < \lambda_p$ are achieved. For the Mach 1.5 case, L_{grad} at the shock front is approximately equal to λ_p in the whole computational domain. For the Mach 3 case, the shock is strong at the cylinder nose region. As the shock bends and extends on both sides, L_{grad} increases from $\lambda_p/2$ at the center ($y = 250$ μm) to $2\lambda_p$ at $y = 50$ μm. A density gradient with $L_{\mathrm{grad}} < \lambda_p$ is achieved in the interval $y = [150\ \mu\mathrm{m}, 350\ \mu\mathrm{m}]$. These density ramps provide a simple and reliable method for threshold controlled and nonthreshold controlled electron self-injection. Moreover, by precisely controlling L_{grad} to be one plasma wave length, the beam quality may be greatly improved for threshold controlled self-injection.

ACKNOWLEDGMENTS

The authors would like to thank Z. M. Sheng and M. Zeng. This work is supported by the National Natural Science Foundation of China (Project No. 11147027) and Anhui Provincial Natural Science Foundation (Project No. 090412030).

[1] T. Tajima and J. M. Dawson, Phys. Rev. Lett. **43**, 267 (1979).
[2] A. Pukhov and J. Meyer-ter-Vehn, Appl. Phys. B **74**, 355 (2002).
[3] I. Kostyukov, A. Pukhov, and S. Kiselev, Phys. Plasmas **11**, 5256 (2004).
[4] J. Faure, Y. Glinec, A. Pukhov, S. Kiselev, S. Gordienko, E. Lefebvre, J.-P. Rousseau, F. Burgy, and V. Malka, Nature (London) **431**, 541 (2004).
[5] C. G. R. Geddes, C. Toth, J. Van Tilborg, E. Esarey, C. B. Schroeder, D. Bruhwiler, C. Nieter, J. Cary, and W. P. Leemans, Nature (London) **431**, 538 (2004).
[6] S. P. D. Mangles, C. D. Murphy, Z. Najmudin, A. G. R. Thomas, J. L. Collier, A. E. Dangor, E. J. Divall, P. S. Foster, J. G. Gallacher, C. J. Hooker, D. A. Jaroszynski, A. J. Langley, W. B. Mori, P. A. Norreys, F. S. Tsung, B. R. Walton, and K. Krushelnick, Nature (London) **431**, 535 (2004).
[7] J. Faure, C. Rechatin, A. Norlin, A. Lifschitz, Y. Glinec, and V. Malka, Nature (London) **444**, 737 (2006).
[8] H. Kotaki, I. Daito, M. Kando, Y. Hayashi, K. Kawase, T. Kameshima, Y. Fukuda, T. Homma, J. Ma, L.-M. Chen, T.-Zh. Esirkepov, A.-S. Pirozhkov, J.-K. Koga, A. Faenov, T. Pikuz, H. Kiriyama, H. Okada, T. Shimomura, Y. Nakai, M. Tanoue, H. Sasao, D. Wakai, H. Matsuura, S. Kondo, S. Kanazawa, A. Sugiyama, and H. Daido, Phys. Rev. Lett. **103**, 194803 (2009).
[9] C. Rechatin, J. Faure, A. Ben-Ismail, J. Lim, R. Fitour, A. Specka, H. Videau, A. Tafzi, F. Burgy, and V. Malka, Phys. Rev. Lett. **102**, 164801 (2009).
[10] H. Suk, N. Barov, J. B. Rosenzweig, and E. Esarey, Phys. Rev. Lett. **86**, 1011 (2001).
[11] T.-Y. Chien, C.-L. Chang, C.-H. Lee, J.-Y. Lin, J. Wang, and S.-Y. Chen, 2002. Phys. Rev. Lett. **94**, 115003 (2005).
[12] J. U. Kim, N. Hafz, and H. Suk, Phys. Rev. E **69**, 026409 (2004).
[13] S. Bulanov, N. Naumova, F. Pegoraro, and J. Sakai, Phys. Rev. E **58**, R5257 (1998).
[14] E. Esarey and M. Pilloff, Phys. Plasmas **2**, 1432 (1995).
[15] C. G. R. Geddes, K. Nakamura, G. R. Plateau, C. Toth, E. Cormier-Michel, E. Esarey, C. B. Schroeder, J. R. Cary, and W. P. Leemans, Phys. Rev. Lett. **100**, 215004 (2008).
[16] A. J. Gonsalves, K. Nakamura, C. Lin, D. Panasenko, S. Shiraishi, T. Sokollik, C. Benedetti, C. B. Schroeder, C. G. R. Geddes, J. van Tilborg, J. Osterhoff, E. Esarey, C. Toth, and W. P. Leemans, Nature Phys. **7**, 862 (2011).
[17] J. Faure, C. Rechatin, O. Lundh, L. Ammoura, and V. Malka, Phys. Plasmas **17**, 083107 (2010).
[18] K. Schmid, A. Buck, C. M. S. Sears, J. M. Mikhailova, R. Tautz, D. Herrmann, M. Geissler, F. Krausz, and L. Veisz, Phys. Rev. ST Accel. Beams **13**, 091301 (2010).
[19] J. D. Anderson, *Fundamentals of Aerodynamics* (McGraw-Hill, Boston, 2001), p. 579, 3rd ed.